TISSUE ENGINEERING: Part A
Volume 19, Numbers 17 and 18, 2013

DOI: 10.1089/ten.tea.2012.0545

Bioengineering Organized, Multilamellar Human Corneal Stromal Tissue by Growth Factor Supplementation on Highly Aligned Synthetic Substrates

Jian Wu, PhD,[1] Yiqin Du, MD, PhD,[2] Mary M. Mann, MS,[2] Enzhi Yang, MS,[2]
James L. Funderburgh, PhD,[2] and William R. Wagner, PhD[1]

Recapitulating the microstructure of the native human corneal stromal tissue is believed to be a key feature in successfully engineering the corneal tissue. The stratified multilayered collagen fibril lamellae with orthogonal orientation determine the robust biomechanical properties of this tissue, and the uniform collagen fibril size and interfibrillar spacing are critical to its optical transparency. The objective of this investigation was to develop a highly organized collagen-fibril construct secreted by human corneal stromal stem cells (hCSSCs) to mimic the human corneal stromal tissue. In culture on a highly aligned fibrous substrate made from poly(ester urethane) urea, the fibroblast growth factor-2 (FGF-2, 10 ng/mL) and transforming growth factor-beta 3 (TGF-β3, 0.1 ng/mL) impacted the organization and abundance of the secreted collagen fibril matrix. hCSSCs differentiated into keratocytes with significant upregulation of the typical gene markers, including *KERA, B3GnT7,* and *CHST6*. FGF-2 treatment stimulated hCSSCs to secrete collagen fibrils strongly aligned in a single direction, whereas TGF-β3 induced collagenous layers with orthogonal fibril orientation. The combination of FGF-2 and TGF-β3 induced multilayered lamellae with orthogonally oriented collagen fibrils, in a pattern mimicking the human corneal stromal tissue. The constructs were 60–70 μm thick and had an increased content of cornea-specific extracellular matrix components, including keratan sulfate, lumican, and keratocan. The approach of combining substrate cues with growth factor augmentation offers a new means to engineer well-organized, collagen-based constructs with an appropriate nanoscale structure for corneal repair and regeneration.

Introduction

Cornea, the transparent outermost layer of the human eye, provides three fundamental functions of the ocular system, including chemical and mechanical protection, transparency for light transmission, and light refraction. Approximately 10 million individuals are estimated to suffer from corneal blindness due to trauma, bacterial and viral infections, and genetic disorders.[1] Corneal transplantation is a conventional approach to correct corneal dysfunction. Although the success of grafting is initially high, long-term survival can be as low as 64%.[2] In addition, cultural factors limit the donor cornea supply in many countries. These limitations have stimulated efforts to develop a fully artificial keratoprostheses to mimic the primary functions of the native human cornea and provide an allograft alternative.[3–5]

The stroma comprises 90% of the corneal thickness and is the major structural component of the cornea. It is comprised of 300–500 layers of aligned collagen fibrils in orthogonal orientations. Each layer is 1–2 μm with a uniform collagen fibril size and spacing. The unique uniform small collagen fibril diameter and regular spacing are principally responsible for corneal optical transparency.[6–8] Stromal keratocytes reside between the collagen layers and are responsible for secretion of the molecular components of the stroma. To develop a biological equivalent of the human corneal stroma, reproducing its unique microstructure and composition appears essential.

In a previous report,[9] we demonstrated topographical cues to be important in initiating and guiding the secretion of organized human corneal stroma-like extracellular matrix (ECM) by human corneal stromal stem cells (hCSSCs). Culture of these cells on a highly aligned fibrous substrate made from poly(ester urethane) urea (PEUU) produced aligned collagen fibrils of uniform size and spacing, within an elaborated ECM of collagen-V, collagen-VI, keratan sulfate, and keratocan. This construct, however, did not stratify into the layers characteristic of native stromal tissue. Further, the thin single-layer constructs (~10 μm) were not amenable to physical stacking in an attempt to create a stromal construct of the thickness and mechanical properties that would be clinically required. These limitations stimulated this investigation

[1]Department of Surgery, McGowan Institute for Regenerative Medicine, University of Pittsburgh, Pittsburgh, Pennsylvania.
[2]Department of Ophthalmology, University of Pittsburgh School of Medicine, Pittsburgh, Pennsylvania.

of growth factor augmentation during the culture period in an effort to increase the thickness and multilamellar features found in native tissue.

The role of identified growth factors in regulating corneal wound healing is well recognized.[10] Specifically, the insulin-like growth factor (IGF), transforming growth factor beta (TGF-β), fibroblast growth factor-2 (FGF-2, also known as basic fibroblast growth factor [bFGF]), and platelet-derived growth factor (PDGF) are examples of factors that significantly influence keratocyte proliferation, migration, differentiation, and morphology. TGF-β isoforms play a crucial role in wound healing of various organs, including the cornea, and induce collagenous ECM secretion by mesenchymal cells.[11] Recently, Hassell and coworkers[12] systematically investigated how these growth factors affected keratocyte synthesis of collagen and proteoglycans, finding that FGF-2 inhibited the synthesis of collagen (type I and type III) and glycosaminoglycans, but stimulated cell proliferation. Zieske and collaborators have shown TGF-β to induce stromal tissue secretion by primary human corneal fibroblasts.[13–16] These constructs were up to 60 μm thick and multilayered. The TGF-β3 was most effective to induce the stromal matrix without expression of fibrotic markers.[16] These findings suggest an effective way to reproduce native corneal stromal tissue with growth factor manipulation. In this report, the effects of FGF-2 and TGF-β3, individually and together, are combined with a highly aligned fibrous substrate in an effort to generate corneal stromal tissue constructs that reflect the structural organization and composition of native tissue, and that are of dimensions that might be considered for further implementation in animal models.

Experiments and Methods

Materials

PEUU was synthesized in the manner of previous reports.[9] The yielded polymer was dissolved in hexafluoroisopropanol (HFIP; Oakwood Products, Inc.) under mechanical stirring at room temperature. Highly aligned fibrous PEUU substrates were prepared by electrospinning onto a rapidly rotating mandrel as described previously.[9] In brief, a 5 wt% HFIP solution of PEUU was fed at 1.0 mL/h by a syringe pump (Harvard Apparatus) into a steel capillary (ID = 0.43 mm) suspended over an aluminum wheel collector 2 cm wide and 20 cm in diameter. A high positive voltage (+10 kV) was applied to the steel capillary containing the polymer solution, and a high negative voltage (−5 kV) was applied to the aluminum collection wheel. PEUU fibrils were collected on the wheel as it rotated at 2000 rpm resulting in fiber alignment. The yielded fibrous substrates were 200 μm thick.

Human corneas unsuitable for transplant were obtained from the Center for Organ Recovery & Education. Two corneas from a 44-year-old donor were used in the experiments. hCSSCs were isolated from collagenase-digested limbal stromal tissue growth at clonal density in a stem cell growth medium (SCGM) containing DMEM/MCDB-201 with 2% fetal bovine serum, 10 ng/mL epidermal growth factor, 10 ng/mL PDGF-BB, 5 μg/mL insulin, 5 μg/mL transferrin, 5 ng/mL selenous acid (ITS), 1 mg/mL AlbuMax, 0.1 mM ascorbic acid-2-phosphate, 10^{-8} M dexamethasone, 100 IU/mL penicillin, 100 μg/mL streptomycin, 50 μg/mL gentamicin, and 100 ng/mL cholera toxin. The characteristics of the cloned stem cells were similar to those of the side-population cells described previously[17] in terms of clonogenicity, keratocytic differentiation, multipotency, and stem cell marker expression. Cells at passage six were used for the experiments as in our previous study.[9]

Primary antibodies used for immunostaining included the anti-keratocan polyclonal peptide antibody (Kera C, a gift from Winston Kao, the University of Cincinnati, Cincinnati OH),[18] the monoclonal antibody J19 to keratan sulfate (a gift from Nirmala SundarRaj, the University of Pittsburgh, Pittsburgh, PA), anti-collagen I (Sigma-Aldrich), anti-collagen V (Chemicon), and anti-collagen VI (Chemicon) monoclonal antibodies. Fluorescently tagged secondary antibodies, Alexa Fluor 488 anti-mouse IgG, Alexa Fluor 546 anti-goat IgG, as well as nuclear dye DAPI were purchased from Invitrogen. In addition, Alexa Fluor 488 phalloidin and calcein AM were also purchased from Invitrogen.

Cell culture

Discs of highly aligned fibrous PEUU substrate were anchored in wells of 24-well culture plates using Silicone Rubber O-rings and sterilized by ultraviolet radiation for 20 min on each side. hCSSCs were seeded on the substratum at 5.0×10^4 cells/cm^2 and incubated with 1.0 mL of SCGM until confluent (usually 3 days).[9]

Differentiation was induced with the keratocyte differentiation medium (KDM) consisting of the advanced DMEM (Invitrogen) supplemented with 1.0 mM L-ascorbic acid-2-phosphate (Sigma-Aldrich), 2 mM L-alanyl-L-glutamine (GlutaMax™-1; Invitrogen), 50 μg/mL gentamicin (Invitrogen), and 100 μg/mL penicillin (Mediatech). KDM was supplemented with (1) 10 ng/mL of the basic FGF-2 (Sigma-Aldrich), (2) 0.1 ng/mL of the TGF-β3 (Sigma-Aldrich), or (3) the FGF-2 (10 ng/mL) + TGF-β3 (0.1 ng/mL) as noted. The medium was changed twice per week for up to 9 weeks.

Two-photon fluorescent microscopy

Multiphoton microscopy was performed using an Olympus FV 1000 multiphoton microscope. This is an upright fixed stage microscope equipped with a large area motorized stage. Specimens were mounted in a home built imaging chamber, and three-dimensional image sets collected with a 25 × 1.0 NA objective specifically designed for multiphoton microscopy. The microscope laser was tuned to 830 nm, which allowed collection of the second harmonic generation (SHG) signal of collagen fibrils. The images were collected as three-dimensional data sets (section spacing 1 μm), with the number of sections in each stack varying from specimen to specimen. Image stacks once collected were processed into three-dimensional stacks using Imaris (Bitplane).

Electron microscopy

Specimens were fixed in cold 2.5% glutaraldehyde (EM grade; Taab Chemical) in 0.1 M phosphate-buffered saline (PBS) pH 7.3. The specimens were rinsed in PBS, postfixed in 1% osmium tetroxide (Electron Microscopy Sciences) with 0.1% potassium ferricyanide (Fisher), and dehydrated through a graded series of ethanol washes. The dehydrated samples were embedded in Epon (Energy Beam Sciences) and ultrathin sections (65 nm) were cut perpendicular to the alignment of the

underlying fibrous substrates. Sections were stained with 2% uranyl acetate (Electron Microscopy Sciences) in a 1:1 mixture of water and methanol, and then with aqueous 1% phosphotungstic acid (Sigma-Aldrich), pH 3.2. The sections were examined and photographed with a Jeol 1011 transmission electron microscope (JEOL Ltd.) working at 80 kV.

Gene expression

Gene expression was determined by quantitative RT-PCR essentially as described previously.[9] Briefly, DNAse-treated total RNA (400 ng) isolated from constructs was transcribed to cDNA using priming with random hexamers. Quantitative PCR of cDNA equivalent to 20 ng RNA was performed with direct dye binding (SYBR Green; Applied Biosystems) according to the manufacturer's instruction. A dissociation curve for each SYBR-based reaction was generated to confirm that there was no nonspecific amplification. Amplification of 18S rRNA was performed for each cDNA (in triplicate) for normalization of the RNA content. Relative mRNA abundance was calculated as the cycle threshold (Ct) for amplification of a gene-specific cDNA minus the average Ct for 18S expressed as a power of 2 ($2^{-\Delta Ct}$). Three individual gene-specific values thus calculated were averaged to obtain a mean ± standard deviation (SD). Primer sequences were previously published.[18]

Whole-mount immunostaining

After 9 weeks of culture, the ECM deposited by hCSSCs on PEUU substrates were fixed in 2.5% paraformaldehyde in PBS at room temperature for 20 min, rinsed in PBS, and stored at 4°C in PBS until further processing. Except in the case of keratocan, for ECM staining, the fixed samples were incubated in 10% heat-inactivated goat serum at room temperature for 1 h to block nonspecific binding, rinsed in PBS, and incubated with mouse monoclonal primary antibodies diluted with 1% bovine serum albumin (BSA; Fluka) in PBS overnight at 4°C in a sealed moist box. For immunostaining of keratocan, the sample was first digested with keratanase (0.5 U/mL) (Sigma Aldrich) in 1% BSA in PBS for 2 h at 37°C, rinsed in PBS, and then incubated with primary goat anti-human keratocan antibody overnight at 4°C, following three washes (10 min each time) with PBS.

For myofibroblast staining, fixed cells were first permeabilized with 0.1% Triton X-100 in PBS for 20 min, and thoroughly washed by PBS. The permeabilized cells were labeled with Alexa Flour 488 phalloidin (2 μg/mL; Invitrogen), and incubated with mouse anti-human α-SMA (1:100; Sigma-Aldrich) overnight at 4°C, and then washed 3 × 10 min with PBS.

The secondary antibody Alexa Fluor 488 donkey anti-mouse or Alexa Fluor 488 donkey anti-goat (1:2500; Invitrogen) together with 4′,6-diamidino-2-phenylindole (DAPI) (0.5 ng/mL; Roche Molecular Biochemicals) was added to the samples, and incubated for 2 h at room temperature. The stained samples were placed in an aqueous mounting medium (Thermo Fisher Scientific) and examined using an Olympus FluoView FV1000 confocal microscope.

Immunoblotting

Proteoglycans in the culture media were isolated and collected using SPEC 3 NH_2-ion exchange columns (Agilent Technologies), dialyzed, and dried as previously described.[19] Portions of each sample were treated with 0.1 U/mL chondroitinase ABC (Sigma-Aldrich) or 0.5 U/mL keratanase (Sigma-Aldrich) overnight at 37°C in 0.1 M ammonium acetate, pH 7.5. Proteins were separated on 4%–20% SDS-PAGE gels (Bio-Rad Laboratories), transferred to the PVDF-FL membrane (Millipore), and detected using immunoblot analysis with specific antibodies. Keratocan was identified with the antibody Kera C, lumican with the monoclonal antibody Lum-1 (provided by Bruce Caterson, Cardiff University, Wales, United Kingdom),[20] decorin with the polyclonal anti-DCN antibody (Sigma-Aldrich), keratan sulfate with the monoclonal antibody J19, and dermatan sulfate with the monoclonal antibody BE123 (Millipore). Primary antibodies were detected with the IRDye-labeled secondary antibody (LI-COR Biosciences), and visualized using the LiCor Odyssey Imager.

Statistical analysis

Statistical comparisons were conducted by one-way ANOVA followed by *post hoc* Newman–Keuls multiple comparison testing to evaluate the influence of the growth factors on gene expression of differentiated hCSSCs and $p < 0.05$ was considered significant. All the results pertaining to the construct thickness, collagen fibril size, and interfibrillar spacing are expressed as mean ± SD.

Results

Cell morphology and viability

The response of hCSSCs to the highly aligned fibrous substrate (Fig. 1a) was evaluated after labeling with the vital dye calcein AM (Invitrogen). Labeled, viable hCSSCs were highly aligned and confluent on the oriented fibrous substrate after 3-day culture in SCGM (Fig. 1b). After achieving confluence, the samples were shifted to the serum-free KDM with growth factor supplementation. Without growth factors, cell viability was low and near complete cell death occurred during the 9 weeks of culture (Fig. 1c, d). Further characterizations were not performed for culture with this condition. Compared with the initially confluent sample (Fig. 1b), the KDM supplemented with the FGF-2 (10 ng/mL) maintained cellular alignment on the substrate (Fig. 1e, f), but did not appear to induce significant proliferation during the culture period. Viable hCSSCs gradually decreased with time (Fig. 1e, f). In the KDM supplemented with the TGF-β3 (0.1 ng/mL), hCSSCs lost the initial organized alignment and elongated morphology (Fig. 1g, h). In contrast to the FGF-2, the TGF-β3 enhanced cell density after 4 weeks of culture (Fig. 1g). If the culture medium was supplemented with both the FGF-2 (10 ng/mL) and TGF-β3 (0.1 ng/mL), there was a synergistic effect on the cell viability and morphology. After 4 weeks of culture, viable cell density not only significantly increased, but the initial highly elongated cell morphology and notable orientation remained as well (Fig. 1i). However, cell viability appeared to decrease when the culture period was extended to 9 weeks.

Cell phenotype and gene expression: hCSSC response to growth factors

In samples treated with the FGF-2 only, f-actin was homogenously distributed near the cell membranes showing

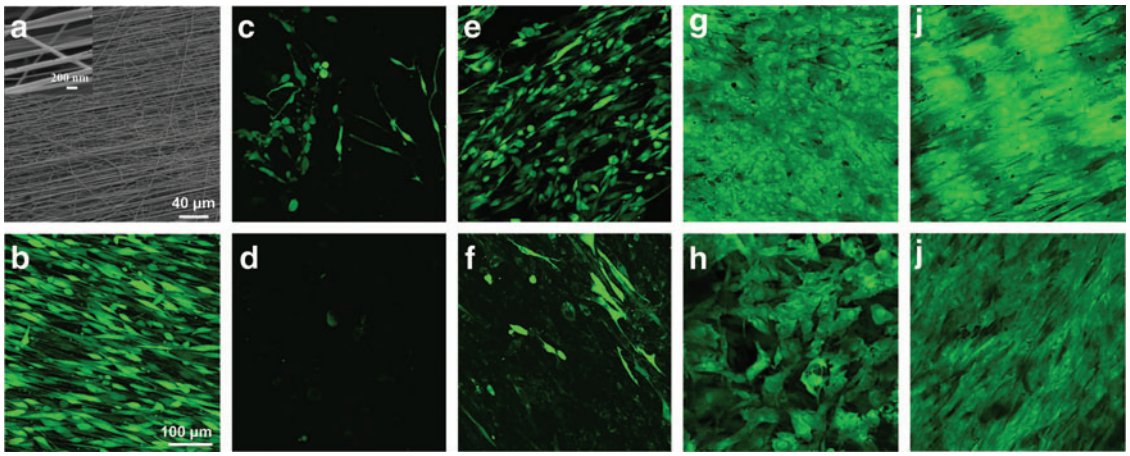

FIG. 1. Cell viability on aligned fibrous substratum in response to growth factors. Scanning electron micrograph of **(a)** aligned fibrous poly(ester urethane) urea (PEUU), and confocal laser-scanning micrograph of **(b)** 100% confluent human corneal stromal stem cells (hCSSCs) on the aligned fibrous substrate before differentiation. Cell viability and morphology of hCSSCs seeded on the highly aligned PEUU substrate with different growth factor treatments after 100% confluence: **(c, d)** no growth factor, **(e, f)** 10 ng/mL fibroblast growth factor-2 (FGF-2), **(g, h)** 0.1 ng/mL transforming growth factor-beta 3 (TGF-β3), and **(i, j)** 10 ng/mL FGF-2 + 0.1 ng/mL TGF-β3 at week 4 **(c, e, g, i)** and week 9 **(d, f, h, j)**. Fluorescent labeling was with the cell viability marker, calcein AM. Color images available online at www.liebertpub.com/tea

few stress fibers crossing the cell body (Fig. 2a). α-SMA staining was also not observed in these samples (Fig. 2d). After treatment with the TGF-β3 only, hCSSCs developed prominent f-actin fibril bundles within the cells (Fig. 2b); however, expression of α-SMA (Fig. 2e) was very weak. Treatment with both the FGF-2 and TGF-β3 appeared to completely inhibit α-SMA expression (Fig. 2f), and weaken the organization of f-actin stress fibers (Fig. 2c).

Figure 3 shows the gene expression patterns of differentiated hCSSCs after 9 weeks of culture with varying growth factor supplementation. Consistent with previous reports,[9,18] hCSSCs in the KDM downregulated *ABCG2*, a marker of stromal stem cells, and substantially upregulated the gene expression of *ALDH* (aldehyde dehydrogenases 3A1), *CHST6* (carbohydrate sulfotransferase 6), *B3GnT7* (UDP-GlcNAc: Gal-beta-1,3-N-acetylglucosaminyltransferase 7), and *KERA* (keratocan), the genes highly upregulated in keratocytes. Additionally, gene expression of *Fn-EDA* (fibronectin extra domain-A) and α-smooth muscle actin (*α-SMA*), expressed in myofibroblasts, of the differentiated hCSSCs were lower than or comparable to those of hCSSCs in the SCGM.

The phenotypes of differentiated hCSSCs were also a function of the growth factors. The TGF-β3 upregulated keratocyte gene expression (i.e., *B3GnT7, CHST6,* and *KERA*) more substantially than the FGF-2. More importantly, the combination of the FGF-2 and TGF-β3 showed a positive synergistic effect in the expression of keratocyte gene markers. The synergistic effect was also reflected in the expression of myofibroblast gene markers, including Fn-EDA and α-SMA. The combination of FGF-2 and TGF-β3 showed

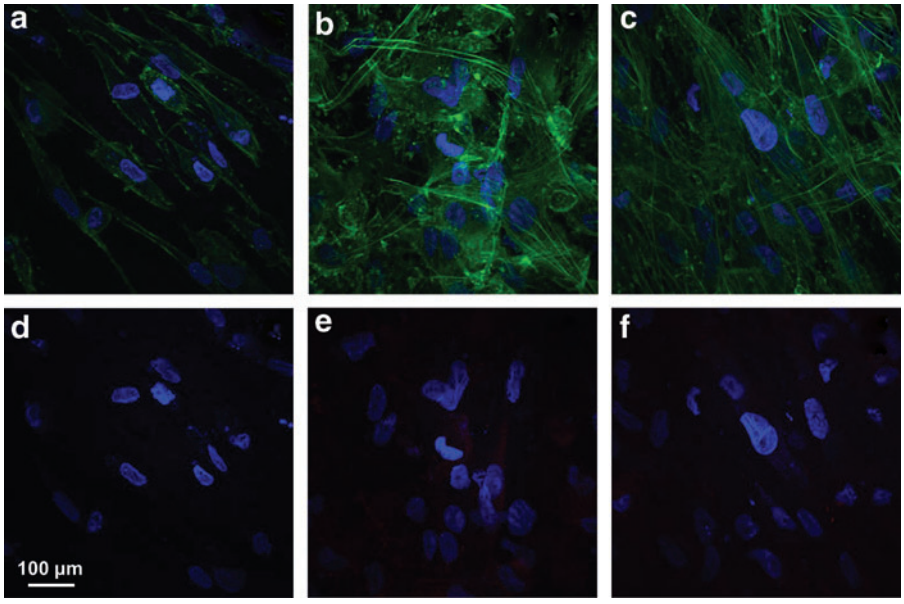

FIG. 2. The cytoskeletal response to growth factor treatment. Cytoskeletal reorganization (green, **a–c)** and expression of α-SMA (red, **d–f)** of hCSSCs treated with **(a, d)** 10 ng/mL FGF-2, **(b, e)** 0.1 ng/mL TGF-β3, and **(c, f)** 10 ng/mL FGF-2 + 0.1 ng/mL TGF-β3. Nuclei were stained by DAPI (blue). Color images available online at www.liebertpub.com/tea

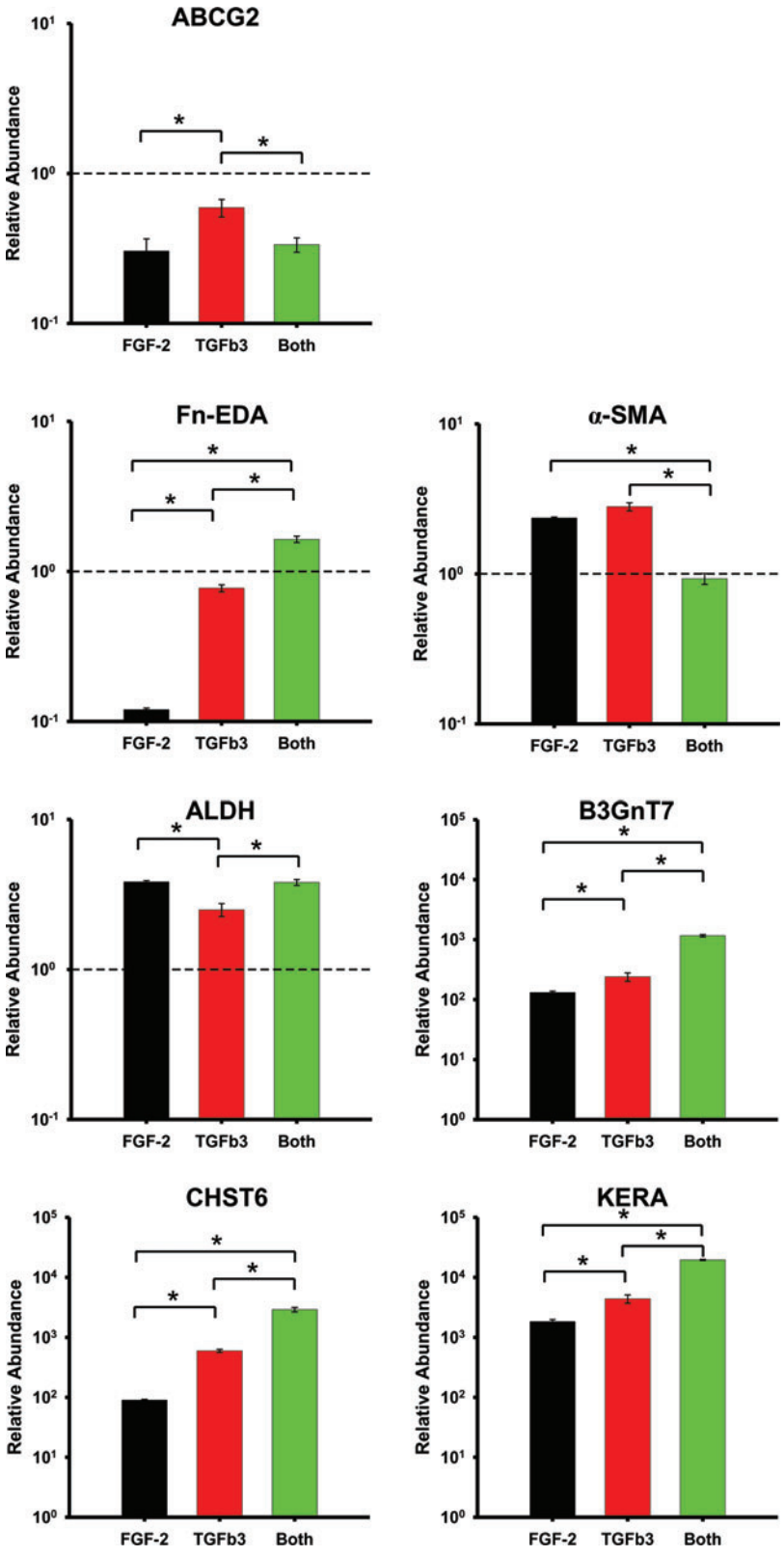

FIG. 3. Gene expression in response to growth factors. Comparison of gene expressions of hCSSCs treated with 10 ng/mL FGF-2 (black), 0.1 ng/mL TGF-β3 (red), and a combination of 10 ng/mL FGF-2 + 0.1 ng/mL TGF-β3 (green). mRNA abundance was normalized with hCSSCs cultured in the stem cell growth medium (SCGM), and expressed in a logarithmic scale. Error bars show standard deviation (SD) of three independent samples. The dashed line represents the expression of hCSSCs cultured in the SCGM. $*p < 0.05$ was considered significant. Color images available online at www.liebertpub.com/tea

more substantial expression of *Fn-EDA* and less *α-SMA* expression than either the FGF-2 or TGF-β3 alone. The expression of *ALDH* was upregulated to a lesser extent with the treatment of the TGF-β3 than with that of either the FGF-2 or both the FGF-2 and TGF-β3.

Microstructures of collagenous construct biosynthesized by hCSSCs

Two-photon micrographs. Highly aligned collagen fibrils feature a second-order nonlinear susceptibility because of

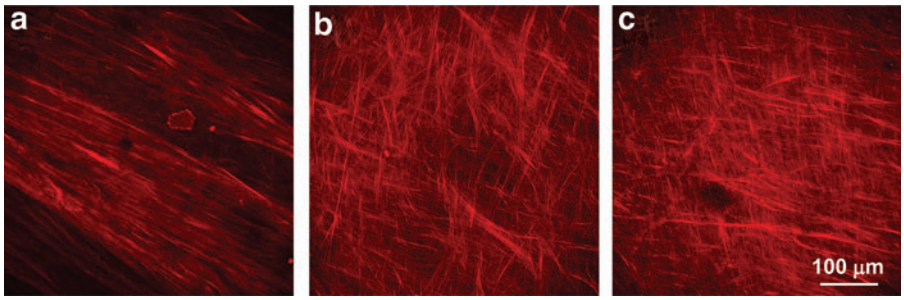

FIG. 4. Two-photon images of hCSSC-secreted collagen on aligned fibrous substrates under treatment with different growth factors. **(a)** 10 ng/mL FGF-2, **(b)** 0.1 ng/mL TGF-β3, and **(c)** 10 ng/mL FGF-2 + 0.1 ng/mL TGF-β3. The second harmonic generation signal for collagen when excited at $\lambda = 830$ nm is red. Color images available online at www.liebertpub.com/tea

structurally high noncentrosymmetry, resulting in a strong SHG.[21–24] Accordingly, the hCSSC-secreted ECM, when examined by two-photon microscopy, showed a very strong SHG signal (Fig. 4). The ECM deposited by hCSSCs on aligned substrates was organized into fibril bundles across the substrate, producing a strong SHG signal. With FGF-2 alone (Fig. 4a), hCSSC-secreted collagen globally aligned in one preferred direction on the aligned PEUU fibrous substrate, as reported in our previous article.[9] In contrast, TGF-β3 treatment resulted in layers of aligned collagen fibrils with orthogonal orientations (Fig. 4b). The combined effects of FGF-2 and TGF-β3 resembled that of TGF-β3 alone in generating multiple layers of aligned fibrils with orthogonal orientation between different layers.

Transmission electron microscopy. The internal microstructure of the collagenous ECM secreted by hCSSCs on the aligned fibrous substrate was investigated by transmission electron microscopy (TEM) after 9 weeks of culture. In sections cut perpendicular to the axis of the PEUU substrate, FGF-2-treated samples (Fig. 5a) showed collagen fibrils perpendicular to the imaging plane. The high level of alignment was consistent with observations from two-photon microscopy. The fibrils formed dense clusters with a uniform fibril size and interfibril spacing. In samples cultured in the TGF-β3, stratified multilayered lamellae were present, showing orthogonal fibril orientation (Fig. 5b). Dense fibril clusters were present with a uniform fibril size and interfibril spacing. In samples treated with both FGF-2 and TGF-β3, the ECM was much more continuous and uniform (Fig. 5c), compared to fibril clusters in the other two culture conditions.

ECM thickness as a function of growth factor supplementation is summarized in Figure 5d. The mean thickness of the ECM secreted by hCSSCs treated with the FGF-2 alone did not significantly differ from that of cells treated with the

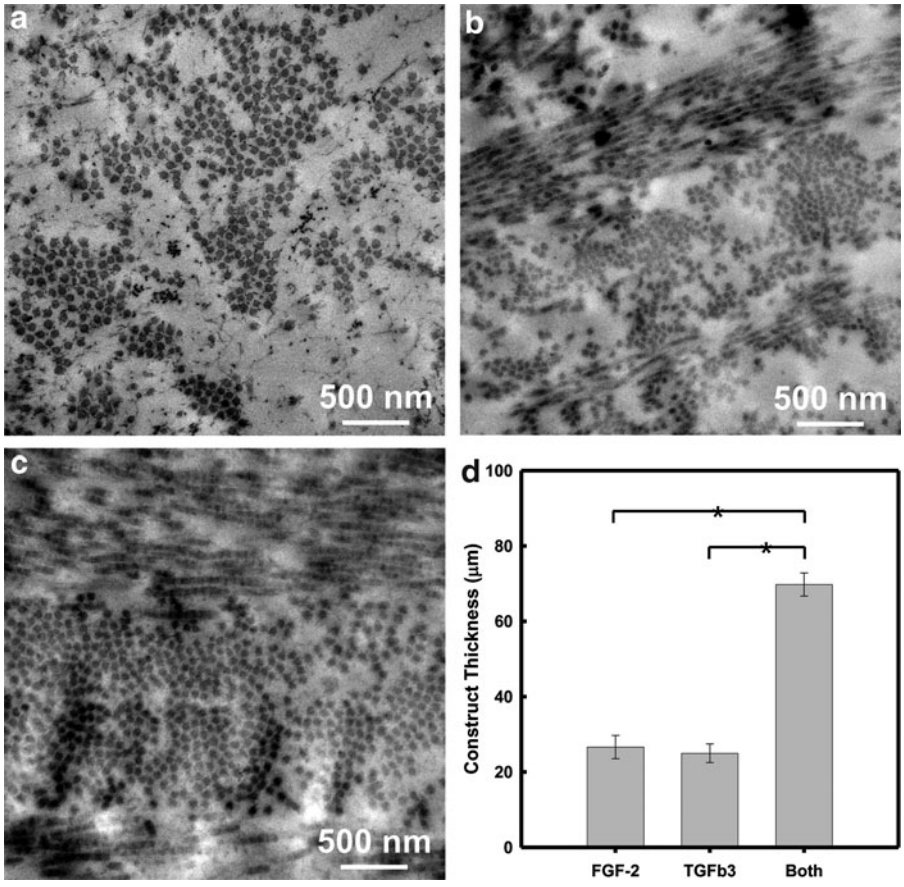

FIG. 5. Transmission electron micrographs of the hCSSC-secreted extracellular matrix (ECM) on the aligned PEUU fibrous substrates varied with growth factor treatment. **(a)** 10 ng/mL FGF-2, **(b)** 0.1 ng/mL TGF-β3, and **(c)** 10 ng/mL FGF-2 + 0.1 ng/mL TGF-β3. The thickness of the ECM secreted by hCSSCs as a function of the growth factor is summarized in **(d)**. $^*p < 0.05$ was considered significant.

TGF-β3 medium alone. However, if hCSSCs were treated with a medium containing both the FGF-2 and TGF-β3, the formed ECM was ~70 μm in thickness, almost three times as thick as that secreted by hCSSCs treated with a medium containing only one of the growth factors.

Figure 6 summarizes the fibril size and interfibril spacing of the secreted collagen as a function of growth factor supplementation. Treatment with the TGF-β3 medium alone induced the smallest fibril diameters and a narrowest size distribution, 37 ± 2.2 nm (Fig. 6c). Supplementation with the FGF-2 medium (Fig. 6a) produced larger fibril diameters and variability, 48.6 ± 4.1 nm. If the culture medium incorporated both the TGF-β3 and FGF-2, the fibril width was reduced and fell between that found for media supplemented with either

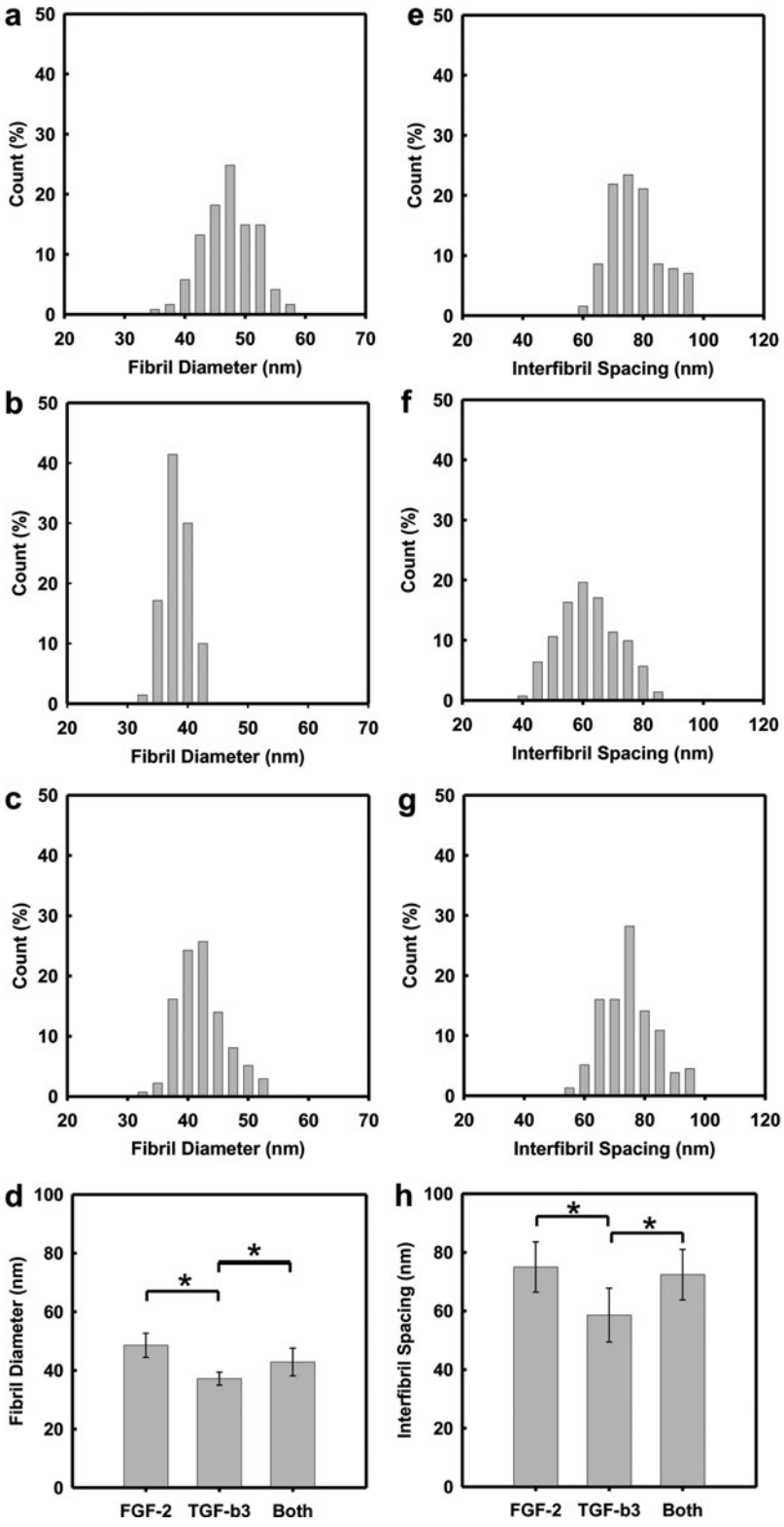

FIG. 6. Digital analysis of the fibril size **(a–c)** and interfibrillar spacing **(e–g)** in the collagen-fibril construct secreted by hCSSCs on the aligned PEUU fibrous substrate with varying growth factor treatments: **(a, e)** 10 ng/mL FGF-2, **(b, f)** 0.1 ng/mL TGF-β3, and **(c, g)** 10 ng/mL FGF-2 + 0.1 ng/mL TGF-β3. The growth factor dependence of the collagen fibril size and interfibrillar spacing is summarized in **(d)** and **(h)**, respectively. Error bars show SD of three independent samples. $*p < 0.05$ was considered significant.

the FGF-2 or TGF-β3 alone. In addition, the dependence of interfibril spacing on growth factor supplementation is similar to that found for the fibril diameter.

ECM protein expression

The expression of collagens and proteoglycans, typifying the unique ECM of human corneal stromal tissue, was examined by whole mount immunohistochemical staining. As shown in Figure 7, the three hCSSC-secreted fibrillar ECMs were not only abundant in type-I collagen, but also exhibited expression of collagen V, collagen VI, keratan sulfate and keratocan, proteins and proteoglycans typically found in native human corneal stromal tissue. In Figure 7a–c, hCSSCs cultured with the FGF-2 were observed to secrete collagen fibrils with one preferred orientation on the highly aligned PEUU fibrous substrate. Interestingly, hCSSCs cultured with TGF-β3 deposited collagen fibrils that appeared to be deposited in two orthogonally aligned orientations (Fig. 7f–h). With both the FGF-2 and TGF-β3 in the culture medium, hCSSCs generated much denser collagen-fibril constructs with orthogonally oriented fibrils, as shown in Figure 7k–m. These results were in accordance with observations from two-photon and TEM. The expression intensity of keratan sulfate and keratocan was also observed to be dependent on the studied growth factors, with the combination of FGF-2 and TGF-β3 resulting in the strongest expression of these ECM components. Comparatively, hCSSCs treated with the FGF-2 secreted the least intensive expression of keratocan and keratan sulfate in the ECM. These results are consistent with the effect of the growth factors on hCSSC gene expression, as shown in Figure 3.

Proteoglycan accumulation in culture media

The corneal stroma contains a family of proteoglycans modified by keratan sulfate that is uniquely present in the cornea and represents markers of tissue differentiation. Decorin and biglycan are dermatan sulfate-containing proteoglycans present in the cornea as well as many other connective tissues. The ratio of keratan sulfate/dermatan sulfate provides a good assessment of keratocyte differentiation.[19,25,26] In culture, these proteoglycans accumulate in the ECM, but are also present in the culture medium.[19] The abundance of keratan sulfate proteoglycans in the conditioned culture medium was assessed by immunoblotting (Fig. 8a–c) showing the characteristic broad molecular weight of this proteoglycan between 100 and 200 kDa.[19] Comparatively, the samples treated with the FGF-2 showed the weakest expression of keratan sulfate (Fig. 8a). The related expression of the samples treated with the TGF-β3 alone was almost independent of time after week 3 (Fig. 8b). When hCSSCs were treated with both the FGF-2 and TGF-β3, keratan sulfate secretion increased with culture time (Fig. 8c). When dermatan sulfate was examined in the same samples (Fig. 8d–f), two bands of distinct molecular sizes were detected. There was little change in the abundance with time in culture. There was no clear difference in the expression of dermatan sulfate between FGF-2-only (Fig. 8d) and TGF-β3-only (Fig. 8e) treatment. However, hCSSCs treated with both the FGF-2 and TGF-β3 appeared to have the lowest dermatan sulfate expression (Fig. 8f). A calculation of the relative ratio of keratan sulfate to dermatan sulfate in each sample (Fig. 8g) shows little change in the ratio for FGF-2-treated cultures. In both cultures exposed to the TGF-β3, the relative

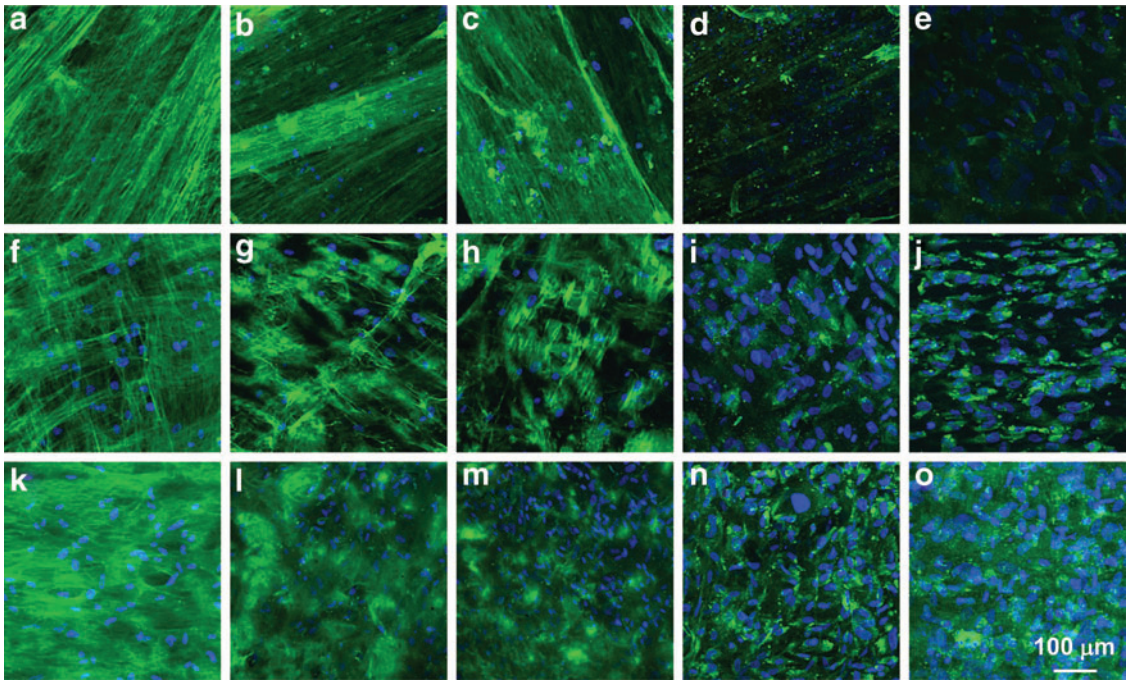

FIG. 7. Immunofluorescent micrographs of the hCSSC-secreted ECM on the aligned PEUU fibrous substrates after 9 weeks of culture varying with growth factor treatments: **(a–e)** 10 ng/mL FGF-2, **(f–j)** 0.1 ng/mL TGF-β3, and **(k–o)** 10 ng/mL FGF-2 + 0.1 ng/mL TGF-β3: **(a, f, k)** collagen I, **(b, g, l)** collagen V, **(c, h, m)** collagen VI, **(d, i, n)** keratan sulfate, and **(e, j, o)** keratocan. Nuclei were stained by DAPI (blue). Color images available online at www.liebertpub.com/tea

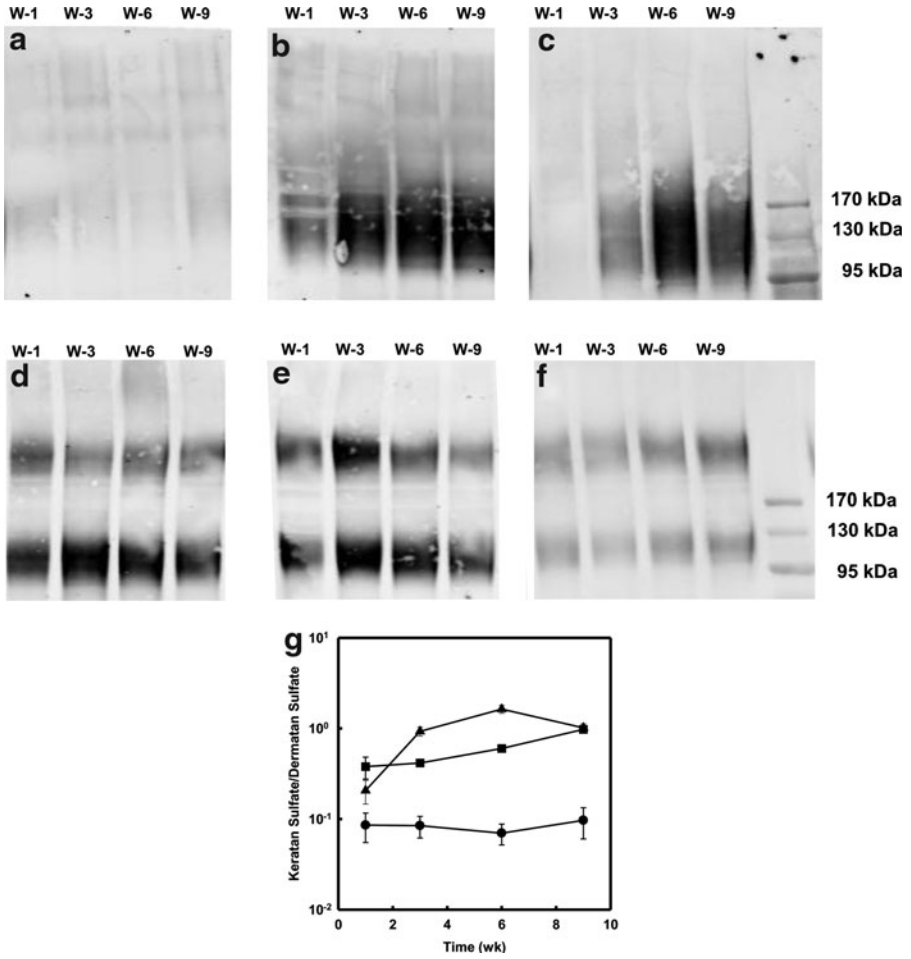

FIG. 8. Immunodetection of corneal proteoglycans in culture media. Keratan sulfate **(a–c)** and dermatan sulfate **(d–f)** in the proteoglycan isolated from culture media of hCSSCs were detected by immunoblotting with the antibody J19 against keratan sulfate glycosaminoglycan chains **(a–c)** and B123 against dermatan sulfate **(d, e, f)** in a medium from cultures treated with **(a, d)** 10 ng/mL FGF-2, **(b, e)** 0.1 ng/mL TGF-β3, and **(c, f)** 10 ng/mL FGF-2 + 0.1 ng/mL TGF-β3. Culture media were collected at week 1 (W-1), week 3 (W-3), week 6 (W-6), and week 9 (W-9), respectively. Digital analysis of the ratios of keratan sulfate to dermatan sulfate are presented **(g)** (●) FGF-2, (■) TGF-β3, and (▲) FGF-2 + TGF-β3.

abundance of keratan sulfate was much higher than in FGF-2 only and both increased dramatically with time, indicating differentiation of the cells to keratocytes. The ratio for cells treated with TGF-β3 alone increased throughout the 9-week incubation, whereas those in the TGF-β3 and FGF-2 peaked at 6 weeks. The highest level of differentiation, based on this ratio, was exhibited by the cultures in both growth factors.

After enzymatic digestion, three core proteins, keratocan, lumican, and decorin, were further assessed by Western blotting (Fig. 9). Decorin, a primary corneal stromal dermatan

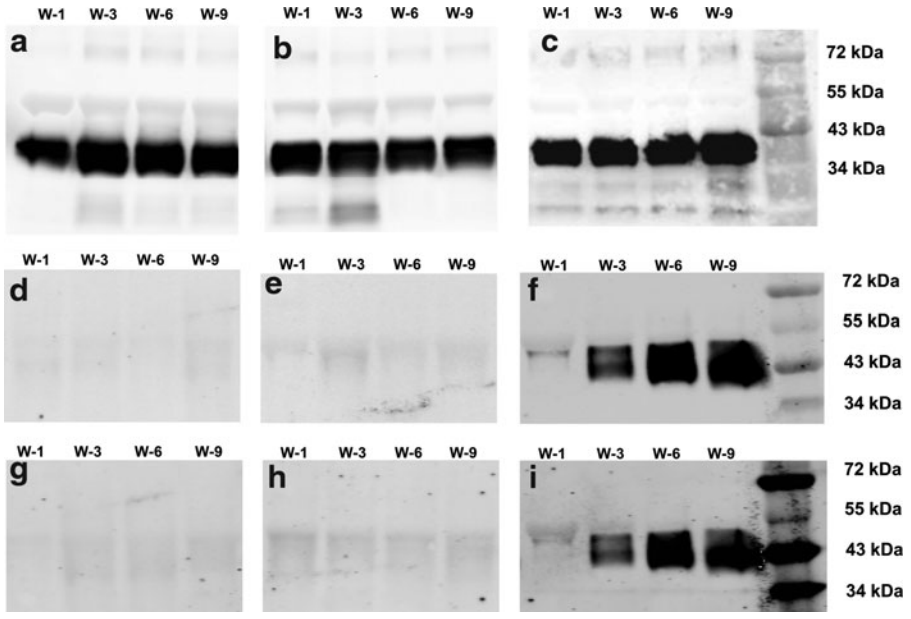

FIG. 9. Western blots of proteoglycan proteins: decorin **(a–c)**, lumican **(c–e)**, and keratocan **(g–i)** recovered from culture media of hCSSCs treated with **(a, d, g)** 10 ng/mL FGF-2, **(b, e, h)** 0.1 ng/mL TGF-β3, and **(c, f, i)** 10 ng/mL FGF-2 + 0.1 ng/mL TGF-β3. These culture media were collected at week 1 (W-1), week 3 (W-3), week 6 (W-6), and week 9 (W-9), respectively.

sulfate proteoglycan exhibited no growth factor dependence and also did not change with time in culture (Fig. 9a–c). Comparatively, the expression of lumican (Fig. 9d, e) and keratocan (Fig. 9g, h), the two core proteins modified with keratan sulfate, was weak in the culture medium supplemented by either the FGF-2 or TGF-β3 alone. However, the expression of these two proteins was much stronger in the samples treated with both the FGF-2 and TGF-β3, and increased with culture time (Fig. 9f, i). The observed effects for the secretion of proteoglycans were in accordance with the gene expression observations shown in Figure 3.

Discussion

Over the past several decades, substantial attention has been given to the development of an artificial cornea to replace the pathologic corneal tissue.[3,27,28] A particularly challenging aspect is to produce bioengineered corneal stromal tissue imbued with biomechanical strength and optical transparency equivalent to the human native corneal stroma. In the current report, we approach stromal tissue engineering utilizing hCSSCs.[9,17,18,29] The ability to generate a highly ordered collagen-fibril-based construct from hCSSCs on an aligned fibrous substrate was demonstrated previously, as was the importance of topographic cues in guiding self-organization of the stromal connective tissue.[9] Although our original construct possessed a dense collagenous matrix with a desirable uniform fibril size and interfibril spacing, it was only ~10 μm thick after 6 weeks of culture and lacked the characteristic stratified, orthogonal multilayers found in the native human corneal stroma. Furthermore, such a thin collagen-fibril construct could not be readily stacked to achieve native tissue thickness (~500 μm). Further optimization of culture conditions was clearly necessary to attempt to recapitulate the process of inducing the hCSSCs to generate the desired ECM content and microstructure.

We previously showed that the FGF-2 had beneficial effects in maintaining the keratocyte phenotype in serum-free cultures[30] and that it was important in inducing keratocyte phenotype and ECM secretion in the absence of attachment to the substratum.[18,31] Similarly, the FGF-2 was observed to be important in induction of keratocyte differentiation of adipose-derived stem cells.[32] Our previous study showing the effect of topographical cues from aligned PEUU fibrous substrates was also carried out in the presence of the FGF-2.[9] The FGF-2 is recognized in its ability to inhibit keratocyte differentiation into myofibroblasts as well as the secretion and deposition of the fibrotic matrix.[30] Our current experiment showed f-actin to be homogeneously distributed around the cell membrane without α-SMA expression for hCSSCs treated with the FGF-2 alone. FGF-2 addition to the culture medium did not alter the elongated cell morphology, but maintained high levels of cell orientation congruent with the highly aligned PEUU fibrous substrate (Fig. 1e, f). The FGF-2 in this serum-free media, however, did not sustain cell viability and expansion of cell numbers over long-term culture.

The TGF-β family members, on the other hand, have been largely associated with the loss of keratocyte phenotypes and induction of fibrotic tissue secretion by corneal cells.[33,34] Most *in vitro* studies have been carried out with the TGF-β1 isoform, which is secreted by inflammatory cells and found in actively healing regions of corneal wounds.[35,36] The TGF-β2 and TGF-β3 isoforms in healing corneas stay associated with corneal cells.[36] The TGF-β3 isoform is responsible for scarless healing of fetal wounds in which the collagen organization is maintained, suggesting it has an *in vivo* biological role distinct from the other two isoforms.[37] Recently, Karamichos *et al*.[16] systematically compared the influence of three isoforms of TGF-β on the expression of fibrotic markers and ECM production by human corneal fibroblasts in an *in vitro* model. Unlike TGF-β1 and TGF-β2, low concentrations of TGF-β3 (0.1 ng/mL) suppressed the expression of fibrotic markers type III collagen and α-SMA. Our data with stem cells in a serum-free model corroborate the ability of the low-dose TGF-β3 to induce a keratocyte-like phenotype. Keratocyte gene expression (Fig. 3) and keratocyte-specific ECM (Fig. 7) were markedly stimulated by the TGF-β3. Additionally, the TGF-β3 did not stimulate myofibroblast formation based on gene expression (Fig. 3) and immunostaining (Fig. 2). Unlike the FGF-2, TGF-β3 had a marked ability to maintain cell density and viability over 9 weeks of culture (Fig. 1g, h).

The TGF-β3 and FGF-2 resulted into two different collagen-fibril constructs: the former led to a stratified collagen-fibril construct with alternating, orthogonally oriented layers, and the latter induced highly oriented collagen fibrils in one preferred direction on the aligned PEUU fibrous substrate. It is not clear what driving force is stimulating the self-organized switching of collagen fibril lamellae to an orthogonal orientation for a subsequent layer. This change correlates with the high level of keratan sulfate-containing proteoglcyans induced by the TGF-β3, but any causality between these events remains speculative.

The effect of combining the FGF-2 with TGF-β appears to be related to the particular isoform of TGF-β. The FGF-2 reduces the myofibroblastic transformation induced by TGF-β1 in corneal cells[38,39] and downregulates expression of lumican and keratocan.[40] The FGF-2 causes an upregulation of TGF-β3 in neural cells[41] and conversely the TFG-β3 can upregulate FGF-2 production,[42] suggesting these growth factors complement one another in an autocrine manner. Together, TGF-β3 and FGF-2 have been reported to stimulate chondrogenesis and collagen production from chondrocytes and mesenchymal bone marrow cells *in vitro*.[43,44] In particular, Kay *et al*.[45] reported the autocrine effect of TGF-β3 and FGF-2 in cell proliferation of corneal stromal fibroblasts.

Incorporating both the FGF-2 and TGF-β3 into the culture medium resulted in several effects on hCSSC behavior that showed evidence of positive synergy, specifically in gene expression of *CHST6, B7GnT7, KERA,* and the expression of lumican and keratocan. Furthermore, keratan sulfate proteoglycans compared to dermatan sulfate protoglcyans reached the highest ratio in the combined growth factors. However, abundance of secreted ECM in the construct was the most dramatic evidence of synergy, with the combined factors inducing as much as a threefold increase in thickness. The final thickness (~70 μm) of these constructs was similar to that achieved by Karamichos *et al.*[16] in the presence of serum. The ability to produce such constructs in a defined medium without serum seems likely to be an advantage if these constructs are to be used therapeutically.

The synergistic effects of the combined growth factors seemed to require at least 3 weeks to achieve a maximum ratio of keratan sulfate to dermatan sulfate (Fig. 8g). This delayed response supports our idea of the ECM as an active participant in the response of the cells to the growth factors. It also suggests the possibility that sequential or cyclic exposure to the FGF-2 and TGF-β3 might be more successful in generating thicker constructs. Elucidation of these temporal effects will be an important priority for subsequent studies.

Corneal stromal cells become myofibroblasts and secrete scar tissue in response to TGF-β isoforms 1 and 2, both *in vitro* and *in vivo*.[34,46] The differential effects of TGF-β3 compared to TGF-β1 and β2 have been reported in several systems *in vivo*, but it remains somewhat of a mystery as to why the TGF- β3 appears to elicit an antifibrotic response, particularly in the presence of the FGF-2. TGF-β proteins localize in the ECM in association with small leucine-rich proteoglycans (SLRPs) such as decorin, biglycan, lumican, and keratocan.[47–49] These interactions can regulate the TGF-β biological activity.[48–50] In an earlier report, we found FGF-2 modulates the type of SLRP molecules secreted by keratocytes[30] and that difference is evidenced here in Figures 8 and 9. We speculate that the complex synergy between the FGF-2 and TGF-β3 observed here may not arise as a unique feature of differential signaling pathways by TGF-β isoforms, but rather from differential interactions of TGF-β3 with corneal SLRP proteoglycans compared to other TGF-β isoforms.

Karamichos *et al*.[16] also demonstrated the influence of isoforms of TGF-β on the fibril size of the collagen-fibril constructs generated by human corneal fibroblasts in the serum-containing medium. Their control group (without TGF-β supplement) had collagen fibril diameters of 25 nm peak. Once treated with the TGF-β3 alone, the peak fibril diameter increased to 37 nm, which was close to our observations. However, in this report, there was no uniform interfibril spacing, which is thought to be essential for corneal transparency.[6–8] To our knowledge, the current work is the first to report the influence of growth factors on both the fibril size and interfibril spacing of constructs secreted and organized by hCSSCs. The fibril size was thought to be determined by the type-I/type-V ratio.[51,52] The observed smaller fibril diameter in the sample treated by the TGF-β3 alone could be due to a smaller ratio of type-I to type-V collagen. The uniform interfibril spacing may have resulted from the abundant cornea-specific SLRP (i.e., keratocan, lumican), as shown in Figures 7–9. The yielded uniform fibril size and interfibril spacing deliver an important message that hCSSCs have a great potential to bioengineer the human corneal stromal equivalent with the appropriate biological cues.

Conclusions

In summary, we show that the organization and properties of the ECM secreted by corneal stromal stem cells on a highly aligned PEUU fibrous template is markedly influenced by the growth factors, FGF-2 and TGF-β3. The FGF-2 induces synthesis of a single layer of collagen fibrils aligned with the fibrous substrate, whereas the TGF-β3 induced distinct orthogonal collagenous layers. The presence of both the FGF-2 and TGF-β3 produced ECM constructs of markedly increased thickness and tightly packed collagen fibrils. The resulting construct comprised of homogeneous stratified lamellae with orthogonally oriented collagen fibrils of uniform fibril size and interfibril spacing containing keratan sulfate proteoglycans, thus mimicking key structural characteristics of the native human corneal stromal tissue. Synergistic cooperation of the FGF and TGF-β family members in controlling the corneal ECM organization is a novel observation in this study. This study provides an important guidance for bioengineering a well-organized, collagen-based construct with an appropriate nanoscale structure for corneal repair and regeneration, and a new approach to recapitulate the overall structural morphology of collagen-fibril constructs by employing growth factor supplementation.

Acknowledgment

The authors would like to thank Dr. Simon C. Watkins, Mr. Gregory Gibson, and Mrs. Ming Sun from the Center of Biologic Imaging (CBI) of University of Pittsburgh for their support and assistance in two-photon microscopy and sample preparation for transmission electronic microscopy. The authors are very grateful for the experimental suggestions from Prof. James D. Zieske (Schepens Eye Research Institute, Harvard Medical School). This work was kindly supported by the Ocular Tissue Engineering and Regenerative Ophthalmology (OTERO) program of the UPMC Eye Center and the McGowan Institute for Regenerative Medicine, Research to Prevent Blindness Inc. NIH grant P30-EY08098 and EY016415 (to J.L.F.).

Disclosure Statement

No competing financial interests exist.

References

1. Whitcher, J.P., Srinivasan, M., and Upadhyay, M.P. Corneal blindness: a global perspective. Bull World Health Organ **79,** 214, 2001.
2. Borderie, V.M., Boelle, P.Y., Touzeau, O., Allouch, C., Boutboul, S., and Laroche, L. Predicted long-term outcome of corneal transplantation. Ophthalmology **116,** 2354, 2009.
3. Griffith, M., Osborne, R., Munger, R., Xiong, X., Doillon, C.J., Laycock, N.L., Hakim, M., Song, Y., and Watsky, M.A. Functional human corneal equivalents constructed from cell lines. Science **286,** 2169, 1999.
4. McLaughlin, C.R., Tsai, R.J., Latorre, M.A., and Griffith, M. Bioengineered corneas for transplantation and *in vitro* toxicology. Front Biosci **14,** 3326, 2009.
5. Fagerholm, P., Lagali, N.S., Merrett, K., Jackson, W.B., Munger, R., Liu, Y., Polarek, J.W., Soderqvist, M., and Griffith, M. A biosynthetic alternative to human donor tissue for inducing corneal regeneration: 24-month follow-up of a phase 1 clinical study. Sci Transl Med **2,** 46ra61, 2010.
6. Maurice, D.M. The structure and transparency of the cornea. J Physiol **136,** 263, 1957.
7. Hart, R.W., and Farrell, R.A. Light scattering in the cornea. J Opt Soc Am **59,** 766, 1969.
8. Benedek, G.B. Theory of the transparency of the eye. Appl Opt **10,** 459, 1971.
9. Wu, J., Du, Y., Watkins, S.C., Funderburgh, J.L., and Wagner, W.R. The engineering of organized human corneal tissue through the spatial guidance of corneal stromal stem cells. Biomaterials **33,** 1343, 2012.

10. Lim, M., Goldstein, M.H., Tuli, S., and Schultz, G.S. Growth factor, cytokine and protease interactions during corneal wound healing. Ocul Surf **1,** 53, 2003.
11. Verrecchia, F., and Mauviel, A. Transforming growth factor-beta and fibrosis. World J Gastroenterol **13,** 3056, 2007.
12. Etheredge, L., Kane, B.P., and Hassell, J.R. The effect of growth factor signaling on keratocytes *in vitro* and its relationship to the phases of stromal wound repair. Invest Ophthalmol Vis Sci **50,** 3128, 2009.
13. Guo, X., Hutcheon, A.E., Melotti, S.A., Zieske, J.D., Trinkaus-Randall, V., and Ruberti, J.W. Morphologic characterization of organized extracellular matrix deposition by ascorbic acid-stimulated human corneal fibroblasts. Invest Ophthalmol Vis Sci **48,** 4050, 2007.
14. Ren, R., Hutcheon, A.E., Guo, X.Q., Saeidi, N., Melotti, S.A., Ruberti, J.W., Zieske, J.D., and Trinkaus-Randall, V. Human primary corneal fibroblasts synthesize and deposit proteoglycans in long-term 3-D cultures. Dev Dyn **237,** 2705, 2008.
15. Karamichos, D., Guo, X.Q., Hutcheon, A.E., and Zieske, J.D. Human corneal fibrosis: an *in vitro* model. Invest Ophthalmol Vis Sci **51,** 1382, 2010.
16. Karamichos, D., Hutcheon, A.E., and Zieske, J.D. Transforming growth factor-beta3 regulates assembly of a non-fibrotic matrix in a 3D corneal model. J Tissue Eng Regen Med **5,** e228, 2011.
17. Du, Y., Funderburgh, M.L., Mann, M.M., SundarRaj, N., and Funderburgh, J.L. Multipotent stem cells in human corneal stroma. Stem Cells **23,** 1266, 2005.
18. Du, Y., Sundarraj, N., Funderburgh, M.L., Harvey, S.A., Birk, D.E., and Funderburgh, J.L. Secretion and organization of a cornea-like tissue *in vitro* by stem cells from human corneal stroma. Invest Ophthalmol Vis Sci **48,** 5038, 2007.
19. Funderburgh, J.L., Mann, M.M., and Funderburgh, M.L. Keratocyte phenotype mediates proteoglycan structure: a role for fibroblasts in corneal fibrosis. J Biol Chem **278,** 45629, 2003.
20. Young, R.D., Swamynathan, S.K., Boote, C., Mann, M., Quantock, A.J., Piatigorsky, J., Funderburgh, J.L., and Meek, K.M. Stromal edema in klf4 conditional null mouse cornea is associated with altered collagen fibril organization and reduced proteoglycans. Invest Ophthalmol Vis Sci **50,** 4155, 2009.
21. Cahalan, M.D., Parker, I., Wei, S.H., and Miller, M.J. Two-photon tissue imaging: seeing the immune system in a fresh light. Nat Rev Immunol **2,** 872, 2002.
22. Zipfel, W.R., Williams, R.M., and Webb, W.W. Nonlinear magic: multiphoton microscopy in the biosciences. Nat Biotechnol **21,** 1369, 2003.
23. Yasui, T., Tohno, Y., and Araki, T. Characterization of collagen orientation in human dermis by two-dimensional second-harmonic-generation polarimetry. J Biomed Opt **9,** 259, 2004.
24. Williams, R.M., Zipfel, W.R., and Webb, W.W. Interpreting second-harmonic generation images of collagen I fibrils. Biophys J **88,** 1377, 2005.
25. Funderburgh, J.L., Hevelone, N.D., Roth, M.R., Funderburgh, M.L., Rodrigues, M.R., Nirankari, V.S., and Conrad, G.W. Decorin and biglycan of normal and pathologic human corneas. Invest Ophthalmol Vis Sci **39,** 1957, 1998.
26. Funderburgh, J.L., and Chandler, J.W. Proteoglycans of rabbit corneas with nonperforating wounds. Invest Ophthalmol Vis Sci **30,** 435, 1989.
27. Minami, Y., Sugihara, H., and Oono, S. Reconstruction of cornea in three-dimensional collagen gel matrix culture. Invest Ophthalmol Vis Sci **34,** 2316, 1993.
28. Zieske, J.D., Mason, V.S., Wasson, M.E., Meunier, S.F., Nolte, C.J., Fukai, N., Olsen, B.R., and Parenteau, N.L. Basement membrane assembly and differentiation of cultured corneal cells: importance of culture environment and endothelial cell interaction. Exp Cell Res **214,** 621, 1994.
29. Pinnamaneni, N., and Funderburgh, J.L. Concise review: stem cells in the corneal stroma. Stem Cells **30,** 1059, 2012.
30. Long, C.J., Roth, M.R., Tasheva, E.S., Funderburgh, M., Smit, R., Conrad, G.W., and Funderburgh, J.L. Fibroblast growth factor-2 promotes keratan sulfate proteoglycan expression by keratocytes *in vitro*. J Biol Chem **275,** 13918, 2000.
31. Funderburgh, M.L., Mann, M.M., and Funderburgh, J.L. Keratocyte phenotype is enhanced in the absence of attachment to the substratum. Mol Vis **14,** 308, 2008.
32. Du, Y., Roh, D.S., Funderburgh, M.L., Mann, M.M., Marra, K.G., Rubin, J.P., Li, X., and Funderburgh, J.L. Adipose-derived stem cells differentiate to keratocytes *in vitro*. Mol Vis **16,** 2680, 2010.
33. Funderburgh, J.L., Funderburgh, M.L., Mann, M.M., Corpuz, L., and Roth, M.R. Proteoglycan expression during transforming growth factor beta -induced keratocyte-myofibroblast transdifferentiation. J Biol Chem **276,** 44173, 2001.
34. Jester, J.V., Barry-Lane, P.A., Petroll, W.M., Olsen, D.R., and Cavanagh, H.D. Inhibition of corneal fibrosis by topical application of blocking antibodies to TGF beta in the rabbit. Cornea **16,** 177, 1997.
35. Huh, M.I., Chang, Y., and Jung, J.C. Temporal and spatial distribution of TGF-beta isoforms and signaling intermediates in corneal regenerative wound repair. Histol Histopathol **24,** 1405, 2009.
36. Huh, M.I., Kim, Y.H., Park, J.H., Bae, S.W., Kim, M.H., Chang, Y., Kim, S.J., Lee, S.R., Lee, Y.S., Jin, E.J., Sonn, J.K., Kang, S.S., and Jung, J.C. Distribution of TGF-beta isoforms and signaling intermediates in corneal fibrotic wound repair. J Cell Biochem **108,** 476, 2009.
37. Soo, C., Beanes, S.R., Hu, F.Y., Zhang, X., Dang, C., Chang, G., Wang, Y., Nishimura, I., Freymiller, E., Longaker, M.T., Lorenz, H.P., and Ting, K. Ontogenetic transition in fetal wound transforming growth factor-beta regulation correlates with collagen organization. Am J Pathol **163,** 2459, 2003.
38. Maltseva, O., Folger, P., Zekaria, D., Petridou, S., and Masur, S.K. Fibroblast growth factor reversal of the corneal myofibroblast phenotype. Invest Ophthalmol Vis Sci **42,** 2490, 2001.
39. Petroll, W.M., Jester, J.V., Barry-Lane, P.A., and Cavanagh, H.D. Effects of basic FGF and TGF beta 1 on F-actin and ZO-1 organization during cat endothelial wound healing. Cornea **15,** 525, 1996.
40. Chen, J., Wong-Chong, J., and SundarRaj, N. FGF-2- and TGF-beta1-induced downregulation of lumican and keratocan in activated corneal keratocytes by JNK signaling pathway. Invest Ophthalmol Vis Sci **52,** 8957, 2011.
41. Reuss, B., Dermietzel, R., and Unsicker, K. Fibroblast growth factor 2 (FGF-2) differentially regulates connexin (cx) 43 expression and function in astroglial cells from distinct brain regions. Glia **22,** 19, 1998.
42. Hildner, F., Peterbauer, A., Wolbank, S., Nurnberger, S., Marlovits, S., Redl, H., van Griensven, M., and Gabriel, C. FGF-2 abolishes the chondrogenic effect of combined BMP-6 and TGF-beta in human adipose derived stem cells. J Biomed Mater Res A **94,** 978, 2010.
43. Hegewald, A.A., Zouhair, S., Endres, M., Cabraja, M., Woiciechowsky, C., Thome, C., and Kaps, C. Towards

biological anulus repair: TGF-beta3, FGF-2 and human serum support matrix formation by human anulus fibrosus cells. Tissue Cell **45,** 68, 2012.
44. Perrier, E., Ronziere, M.C., Bareille, R., Pinzano, A., Mallein-Gerin, F., and Freyria, A.M. Analysis of collagen expression during chondrogenic induction of human bone marrow mesenchymal stem cells. Biotechnol Lett **33,** 2091, 2011.
45. Kay, E.P., Lee, M.S., Seong, G.J., and Lee, Y.G. TGF-βs stimulate cell proliferation via an autocrine production of FGF-2 in corneal stromal fibroblasts. Curr Eye Res **17,** 286, 1998.
46. Jester, J.V., Barry-Lane, P.A., Cavanagh, H.D., and Petroll, W.M. Induction of alpha-smooth muscle actin expression and myofibroblast transformation in cultured corneal keratocytes. Cornea **15,** 505, 1996.
47. Baker, S.M., Sugars, R.V., Wendel, M., Smith, A.J., Waddington, R.J., Cooper, P.R., and Sloan, A.J. TGF-beta/extracellular matrix interactions in dentin matrix: a role in regulating sequestration and protection of bioactivity. Calcif Tissue Int **85,** 66, 2009.
48. Nikitovic, D., Chalkiadaki, G., Berdiaki, A., Aggelidakis, J., Katonis, P., Karamanos, N.K., and Tzanakakis, G.N. Lumican regulates osteosarcoma cell adhesion by modulating TGFbeta2 activity. Int J Biochem Cell Biol **43,** 928, 2011.
49. Boivin, W.A., Shackleford, M., Vanden Hoek, A., Zhao, H., Hackett, T.L., Knight, D.A., and Granville, D.J. Granzyme B cleaves decorin, biglycan and soluble betaglycan, releasing active transforming growth factor-beta1. PLoS One **7,** e33163, 2012.
50. Dellett, M., Hu, W., Papadaki, V., and Ohnuma, S. Small leucine rich proteoglycan family regulates multiple signalling pathways in neural development and maintenance. Dev Growth Differ **54,** 327, 2012.
51. Birk, D.E., Fitch, J.M., Babiarz, J.P., Doane, K.J., and Linsenmayer, T.F. Collagen fibrillogenesis *in vitro*: interaction of types I and V collagen regulates fibril diameter. J Cell Sci **95 (Pt 4),** 649, 1990.
52. Birk, D.E. Type V collagen: heterotypic type I/V collagen interactions in the regulation of fibril assembly. Micron **32,** 223, 2001.

Address correspondence to:
William R. Wagner, PhD
McGowan Institute for Regenerative Medicine
University of Pittsburgh
450 Technology Drive, Suite 300
Pittsburgh, PA 15204

E-mail: wagnerwr@upmc.edu

Received: September 7, 2012
Accepted: April 1, 2013
Online Publication Date: May 13, 2013